Journal on Electronic and Automation Engineering

Vol: 4(1), March 2025

REST Publisher; ISSN: 2583-6951 (Online)

Website: https://restpublisher.com/journals/jeae/

DOI: https://doi.org/10.46632/jeae/4/1/3

Active Damping of Filter Based Dab Converter for CC-CV Controlled EV Fast Charging Applications

***B.N. Prasad, V. Amarnath Reddy, Vaddemani Pavan Kumar Reddy**

Annamacharya Institute of Technology & Sciences (Autonomous) Kadapa, Andhra Pradesh, India

*Corresponding Author Email: bingimalla.n.prasad@gmail.com

Abstract: *Dual Active Bridge (DAB) converter is well suited for off-board fast Electric Vehicle Charging Stations (EVCS) and in DC microgrid-connected EVCS applications. However, proper modification in DAB converter topology is crucial for fast charging, as the charging current is very high, and any oscillations would shorten the EV battery life. As per literature, DAB converter topology integrated with a series inductor at the output for EV battery charging reduces the output current ripple by 40%. Therefore, the equipment needs energy storage. The battery has an important role in energy storage with the performance of the battery that needs attention. The method and type of battery used must be considered to maintain battery lifetime and reduce overcharging. The purpose of this research is to understand the process of fast charging using the CC-CV (Constant Current Constant Voltage) method on Lithium-Ion batteries which is expected to reduce battery overcharging. In this method, the current is maintained constant until certain conditions then followed by constant voltage to prevent overcharging. The voltage from the solar panel is very high, voltage reduction is needed as the charging voltage for the battery.*

1. INTRODUCTION

The Dual Active Bridge (DAB) converter has gained significant attention in the context of off-board fast Electric Vehicle Charging Stations (EVCS) and DC microgrid-connected EVCS applications due to its high efficiency, bidirectional power flow, and inherent capability to handle large power levels. However, to fully capitalize on its potential in fast charging, modifications to the traditional DAB converter topology are necessary. This is due to the nature of fast charging, where high charging currents are required, which can introduce oscillations that, if not properly controlled, can negatively affect the lifespan of the EV battery. One of the critical challenges is ensuring minimal current ripple during the charging process, which could otherwise degrade battery performance and shorten its operational life.

Optimizing DAB Converter Topology for Fast Charging:

To address the issue of current ripple, recent research has shown that integrating a **series inductor** at the output of the DAB converter can significantly reduce the ripple in the output current. This technique has been found to reduce current ripple by as much as **40%**, making it a highly effective solution for EV battery charging. The inductor helps to smooth out the variations in the current, ensuring that the battery receives a more consistent and stable charging current, which is crucial for long-term battery health.
Reducing ripple is important because **current fluctuations** can cause **stress** on the battery, leading to overheating, overcharging, and potentially shortening the battery's overall lifespan. The integration of the series inductor ensures that the converter can maintain a stable output current, making it more suitable for applications such as fast-charging stations, where high-power demands are common.

Energy Storage and Battery Management:

In the context of EVCS, the energy storage system—which is typically a battery—plays a central role in the overall charging performance. Proper battery selection and management are essential not only for the charging process but also for the long-term performance of the battery. In fast-charging scenarios, the high charge current can lead to thermal and chemical stresses in the battery if not properly managed. To prevent this, the battery management system (BMS) must be designed to ensure that the charging process is controlled to minimize overcharging,

overheating, and capacity degradation. Battery selection is a critical factor, with Lithium-Ion (Li-ion) batteries being the most common choice for electric vehicles due to their high energy density, long cycle life, and relatively low self-discharge rates. However, even Li-ion batteries require careful charging to avoid issues such as overcharging or deep discharging, both of which can negatively impact battery performance and lifespan.

The CC-CV Charging Method for Lithium-Ion Batteries:

One of the most widely used methods to ensure safe and efficient charging of Lithium-Ion batteries is the Constant Current-Constant Voltage (CC-CV) charging method. This method addresses the challenges of fast charging by providing an efficient balance between charge rate and battery safety.

- Constant Current (CC) Phase: In this phase, the battery is charged with a constant current, which ensures that the battery charges at a fixed rate. During the CC phase, the current remains constant, and the battery voltage gradually increases. However, there is a predefined threshold voltage at which the CC phase must be transitioned to the CV phase to avoid overcharging.
- Constant Voltage (CV) Phase: Once the battery voltage reaches a certain threshold (typically near the battery's nominal voltage), the charger switches to the constant voltage mode. In the CV phase, the voltage remains constant, and the current gradually decreases as the battery becomes fully charged. This ensures that the battery voltage does not exceed safe levels, preventing overcharging, which can lead to overheating, capacity loss, and potential safety issues.

This CC-CV method not only maximizes the charging efficiency but also minimizes the risk of overcharging, thereby improving battery health and lifespan. It is particularly well-suited for fast-charging applications, where maintaining a high charging rate while ensuring battery safety is essential.
Challenges in Voltage Reduction and Solar Energy Integration

In a typical EVCS powered by renewable energy sources, such as solar panels, the voltage generated from the solar panels is often much higher than the required charging voltage for the battery. For instance, a solar array may produce a voltage in the range of 300V to 600V, whereas most Li-ion batteries used in electric vehicles typically operate with a voltage range of 3.2V to 4.2V per cell (with multiple cells connected in series to achieve higher voltage levels). To bridge this voltage mismatch, a voltage reduction stage is required to step down the high voltage from the solar panels to a level that is safe and compatible with the battery charging specifications. This can be accomplished through various techniques, such as using DC-DC converters or transformers integrated into the charging station, which efficiently reduce the voltage while ensuring minimal loss of power. In the context of solar-powered EVCS, the DAB converter's inherent bidirectional power flow capability makes it particularly advantageous. It allows for efficient power conversion from the solar array to the battery, while also being capable of feeding power back into the grid or microgrid when excess solar energy is available.

2. MATHEMATICAL MODELING OF THE EXISTING DAB TOPOLOGY

A mathematical model of the existing DAB topology is derived using GAM and AOCLM techniques. It is assumed that the effect of equivalent series resistance (ESR) of the output capacitor is zero. Note that GAM is a complex modelling technique and provides a 4th order model. However, it offers additional insights into the dynamics of the converter On the contrary, the AOCLM model is simple and provides a 1 st order model. It is developed by ignoring the non-linear terms of the coupling inductor current. A comparative analysis of both these techniques is presented to evaluate the performance of the DAB converter for EV battery load.

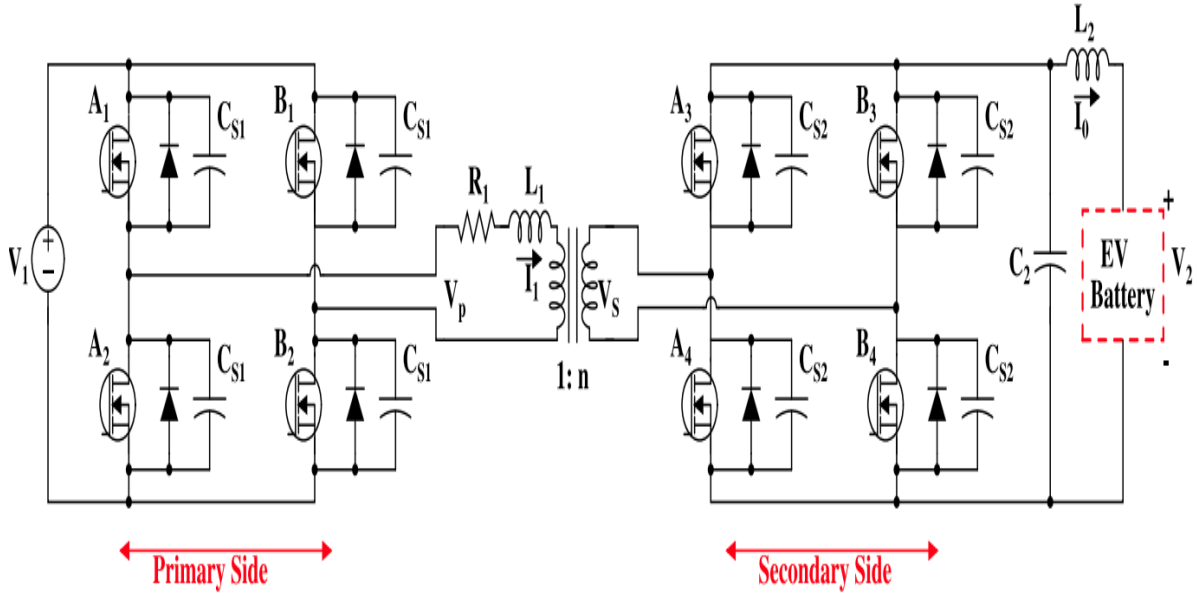

(a)

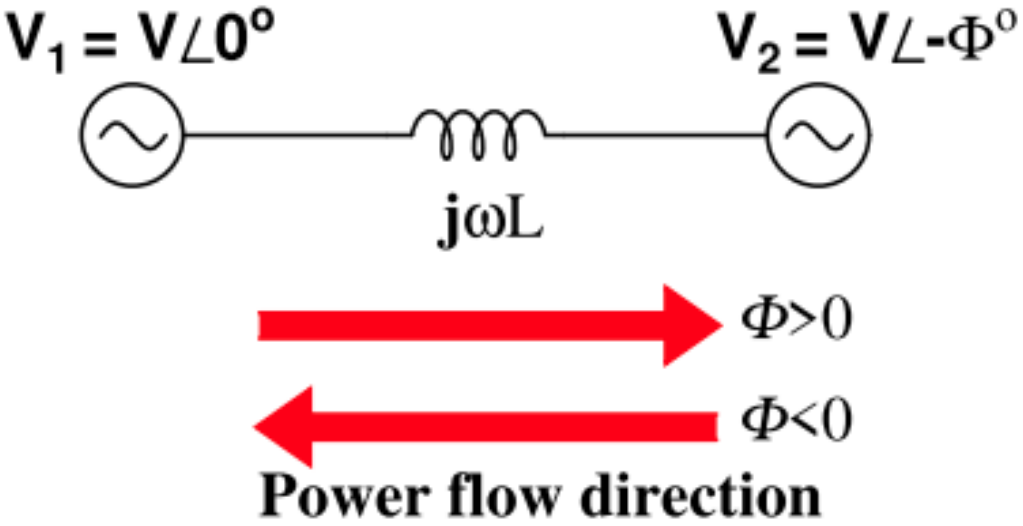

(b)

FIGURE 1. (a) DAB converter conventional topology (b) Operating principle.

3. GENERALIZED AVERAGE MODELING (GAM)

GAM considers time-dependent expansion of the Fourier series [44]. It is based on the fact that approximation of any arbitrary signal y(τ) over the period (t−Ts, t) to some random precision can be carried out using Fourier series, represented as:

$$y(\tau) = y(t - T_s + s) = \sum_k \langle y \rangle_k(t)\, e^{jk\omega_s(t-T_s+s)}$$

where, s ∈ (0, Ts], ωs = 2π/Ts , τ = t − Ts + s. Also, ⟨y⟩k (t) is a complex Fourier or index-k coefficient [45], which is a function of time, expressed as:

$$\langle y \rangle_k(t) = \frac{1}{T_s} \int_0^{T_s} y(t - T_s + s)\, e^{-jk\omega_s(t-T_s+s)} ds$$

Consider, a switched converter model with the switching function u(t) having period Ts , described by

$$\frac{d}{dt} y(t) = f(y(t), u(t))$$

GAM is obtained by computing the average value of the above differential equation. The Fourier coefficient for the state variable is given by,

$$\left\langle \frac{d}{dt} y \right\rangle_k = \langle f(y, u) \rangle_k$$

GAM retains more terms of Fourier series coefficients, which provide more insights into the converter dynamics. For simplicity, the index 0 coefficient is used for the states with slowly varying behavior and index 1 for those with sinusoidal behavior. With only the index 0 terms, the modeling gets reduced to conventional state-space averaging. The ripple component's impact on the average values can be shown by the index 1 term of the switching function and state variables [46], [47].

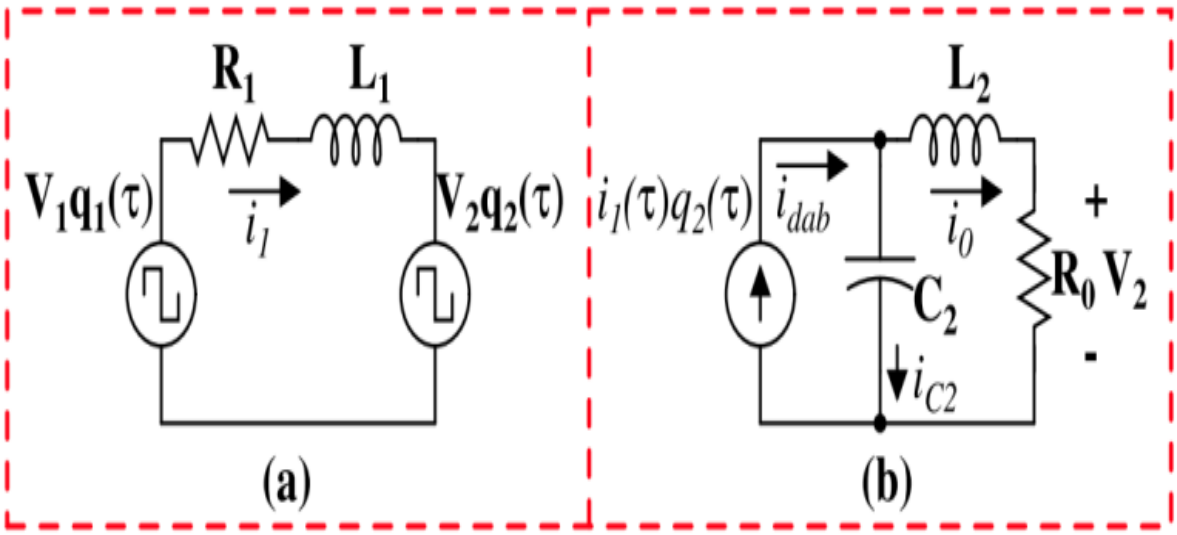

FIGURE 2. DAB equivalent circuit with GAM depicting the (a) Primary side and (b) Secondary side of the converter.

The equivalent circuit of the DAB converter for GAM is shown in Fig. 2. The voltage across the primary and secondary bridge depends on the voltages V1 and V2 as well as the switching functions q1(τ) and q2(τ), respectively. Considering the capacitor voltage and current through the inductors (L1 and L2) as the state variables and applying Kirchhoff's law, we obtain:

$$\frac{d}{dt} i_1(\tau) = \frac{V_1}{L_1} q_1(\tau) - \frac{R_1}{L_1} i_1(\tau) - \frac{V_2}{L_1} q_2(\tau)$$

$$\frac{d}{dt} V_2(\tau) = \frac{i_1(\tau) q_2(\tau)}{C_2} - \frac{i_0(\tau)}{C_2}$$

$$\frac{d}{dt} i_0(\tau) = \frac{V_2(\tau)}{L_2} - \frac{R_0 i_0(\tau)}{L_2}$$

Equations (5) - (7) are non-linear as well as time-varying. Thus, averaging is used to achieve a linear and time-invariant model. The switching functions q1(τ) and q2(τ) are given by:

$$q_1(\tau) = \begin{cases} +1, & 0 \le \tau < \dfrac{T_s}{2}, \\ -1, & \dfrac{T_s}{2} \le \tau < Ts \end{cases}$$

$$q_2(\tau) = \begin{cases} +1, & \dfrac{dT_s}{2} \le \tau < \dfrac{T_s}{2} + \dfrac{dT_s}{2} \\ -1, & \dfrac{T_s}{2} + \dfrac{dT_s}{2} \le \tau < T_s \end{cases}$$

Where Ts = 1/fs is the switching period, d = φ/π, and τ = t − Ts + s. We use single-phase shift modulation: 1) The voltage at the transformer primary, Vp, has two states: a) +V1: A1, B2 ON, b) −V1: A2, B1 ON. Thus, Vp can be given by,

$$V_p(\tau) = q_1(\tau)V_1(\tau)$$

Similarly, the voltage at the transformer secondary, Vs, has two states: a) +V2: A3, B4 ON, b) −V2: A4, B3 ON. Hence, Vs can be given by,

$$V_s(\tau) = q_2(\tau)V_2(\tau)$$

The Fourier coefficients of switching functions q1(τ) and q2(τ) are computed by considering 50% duty ratio, as given below:

$$\langle q_1\rangle_0 = \langle q_2\rangle_0 = 0$$

$$\langle q_1\rangle_1^R = 0$$

$$\langle q_1\rangle_1^I = \frac{-2}{\pi}$$

$$\langle q_2\rangle_1^R = \frac{-2}{\pi} Sin(d\pi)$$

$$\langle q_2\rangle_1^I = \frac{-2}{\pi} Cos(d\pi)$$

By applying the generalized averaging to (5),(6), and (7), and utilizing the complex conjugate, differentiation, and convolution properties of Fourier series, as well as substituting the Fourier coefficients of the switching functions obtained in (12) - (16), the index 0 and 1 averages are calculated, resulting in the derivation of a large signal generalized average model as presented in (17).

$$\begin{bmatrix} i_{1_1R} \\ i_{1_1I} \\ v_{2_0} \\ i_{0_0} \end{bmatrix} = \begin{bmatrix} \frac{-R_1}{L_1} & \omega_s & \frac{2SinD\pi}{\pi L_1} & 0 \\ -\omega_s & \frac{-R_1}{L_1} & \frac{2CosD\pi}{\pi L1} & 0 \\ \frac{-4SinD\pi}{\pi C_2} & \frac{-4CosD\pi}{\pi C_2} & 0 & \frac{-1}{C_2} \\ 0 & 0 & \frac{1}{L_2} & \frac{-R_0}{L_2} \end{bmatrix} \begin{bmatrix} i_{1_1}^R \\ i_{1_1}^I \\ v_{2_0} \\ i_{0_0} \end{bmatrix} + \begin{bmatrix} 0 \\ \frac{-2}{\pi L_1} \\ 0 \\ 0 \end{bmatrix} V_1$$

A Small Signal Model (SSM) representing the converter's dynamic response towards the deviations in the control signal is derived for designing the controller and conducting a stability study of the closed-loop system.

In the event of perturbations in the state variable, the magnitude of i1 1R, i1 1 I, v20 and i00 will deviate from the steady state values. By perturbing the variable of interest followed by linearization, the steady state and small signal variables from the large signal model can be extracted to produce the SSM. In SSM, the state variables in capital letter refer to the steady state, and the perturbations are identified by including '^' on top. We assume perturbations in the input voltage V1 to be zero. We use sine and cosine small angle approximations, i.e. Cos(πd^) = 1 and Sin(πd^) = πd^, to obtain the linearized equations as follow: -

$$Sin\pi(D + \hat{d}) = Sin\pi D + \pi\hat{d}Cos\pi D$$

$$Cos\pi(D + \hat{d}) = Cos\pi D - \pi\hat{d}Sin\pi D$$

$$\begin{bmatrix} \hat{i}_{1_1}^{R} \\ \hat{i}_{1_1}^{I} \\ \hat{v}_{2_0} \\ \hat{i}_{0_0} \end{bmatrix} = \begin{bmatrix} \frac{-R_1}{L_1} & \omega_s & \frac{2SinD\pi}{\pi L_1} & 0 \\ -\omega_s & \frac{-R_1}{L_1} & \frac{2CosD\pi}{\pi L_1} & 0 \\ \frac{-4SinD\pi}{\pi C_2} & \frac{-4CosD\pi}{\pi C_2} & 0 & \frac{-1}{C_2} \\ 0 & 0 & \frac{1}{L_2} & \frac{-R_0}{L_2} \end{bmatrix} \begin{bmatrix} \hat{i}_{1_1}^{R} \\ \hat{i}_{1_1}^{I} \\ \hat{v}_{2_0} \\ \hat{i}_{0_0} \end{bmatrix} + \begin{bmatrix} \frac{2CosD\pi}{L_1} V_{2_0} \\ \frac{-2SinD\pi}{L_1} V_{2_0} \\ \frac{-4}{C_2}((CosD\pi) I_{1_1}^{R} - (CosD\pi) I_{1_1}^{I}) \\ 0 \end{bmatrix} \hat{d}$$

Using SSM as shown in (20), the relation between the variation of phase shift for the designed DAB converter to the variation in requisite state variables, i.e., battery voltage δV2, and current δio, is derived.

4. AVERAGE OUTPUT CURRENT LINEARIZATION MODEL (AOCLM)

The AOCLM is developed by ignoring the non-linear terms of the coupling inductor current. The equivalent circuit for the AOCLM is shown in Fig. 3. The power output of DAB depends on the phase shift angle, φ, given by:

$$P = \frac{nV_1V_2\phi(1-\frac{\phi}{\pi})}{2\pi^2 L_1 f_s}$$

From (21), it can be concluded that the relation between idab and φ is non-linear. Average output current of the DAB (idab) is given by,

$$i_{dab} = \frac{V_1\phi(1-\frac{\phi}{\pi})}{2n\pi L_1 f_s}$$

By perturbing and linearizing (22), we obtain

$$\triangle i_{dab}(t) = \frac{V_1}{2n\pi L_1 f_s}\left(1-\frac{2\phi}{\pi}\right)\triangle\phi(t)$$

Applying KCL to the equivalent circuit in Fig. 3 and substituting in (23), the output-voltage to phase-shift transfer function (TF) becomes:

$$\frac{V_2(s)}{\phi(s)} = \frac{V_1}{2n\pi L_1 f_s}\left(1-\frac{2\phi}{\pi}\right)\frac{sL_2+R_0}{s^2C_2L_2+sC_2R_0+1}$$

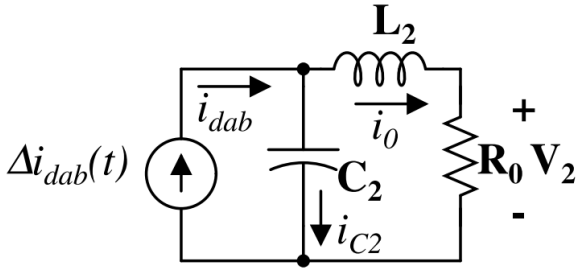

FIGURE 3. DAB equivalent circuit with AOCLM.

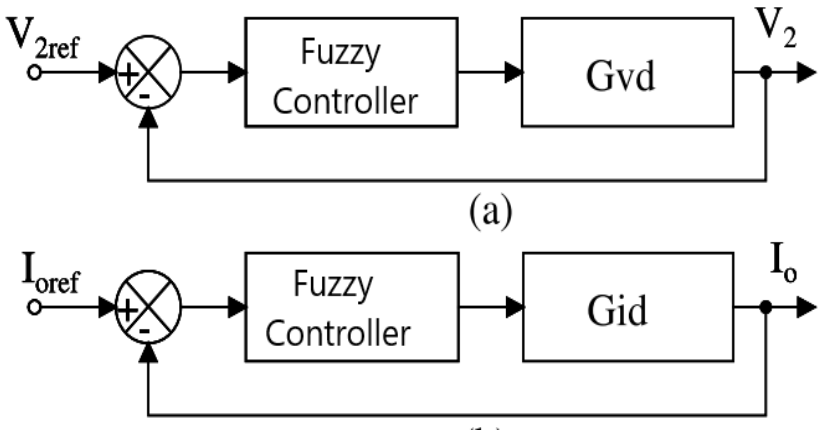

FIGURE 4. Closed-loop model of DAB for (a) Current control (b) Voltage control.

Similarly, output-current to phase-shift TF is calculated as:

$$\frac{i_0(s)}{\phi(s)} = \frac{V_1}{2n\pi L_1 f_s}\left(1 - \frac{2\phi}{\pi}\right)\frac{1}{s^2 C_2 L_2 + sC_2 R_0 + 1}$$

5. CONTROLLER DESIGN AND STABILITY ANALYSIS

Both the GAM and AOCLM with controller exhibit a resonant peak caused by the presence of a pole at the origin in the open-loop TF of the system, resulting in increased rise time (tr). The peak in switching frequency can be linked to the existence of zeros along the imaginary axis in the GAM. Thus, charging the battery at high currents and voltages, particularly during fast charging, will significantly reduce its lifespan. Compared to GAM, AOCLM presents a simple, more accurate and second-order model, and thus we have chosen AOCLM for the voltage and current controller design. Proposed Controller

Fuzzy Controller in Dual Active Bridge (DAB) Converter for Fast Charging

In the context of **fast charging systems** for Electric Vehicle Charging Stations (EVCS), a **Fuzzy Logic Controller (FLC)** can play a critical role in managing the charging process. The DAB converter, in particular, benefits from fuzzy control due to its ability to handle uncertainties and nonlinearities in the system, such as fluctuating input power (e.g., from solar panels) and varying load conditions (e.g., battery state of charge). A **fuzzy controller** can dynamically adjust the control signals for the converter's operation to optimize the charging process, maintain battery health, and minimize charging time.

Why Use Fuzzy Logic Control?

Fuzzy logic is advantageous in power electronic systems like DAB converters because it does not require precise mathematical models of the system. Instead, it uses linguistic variables and fuzzy rules to make decisions based on imprecise inputs, making it suitable for systems with complex and uncertain dynamics. In a fast charging environment, these uncertainties can arise from:

- Variable battery conditions, such as temperature and charge state.
- Changing input power from renewable sources like solar panels.
- System non-linearities, such as variations in power demand or the DAB converter's efficiency.
- Fuzzy logic can be used to control several aspects of the DAB converter, such as current, voltage, or power regulation during the charging process.

Fuzzy Logic Controller Design for DAB Converter

The design of the fuzzy controller typically involves the following components:

Input Variables:
The fuzzy controller receives input from key system parameters. For fast EV charging, common inputs include:

- Battery Voltage (V**)**: Indicates the current charge level of the battery.
- Battery Current (I)**:** Indicates the charging current.
- Error (e)**: T**he difference between the desired voltage and the actual voltage.
- Change in Error (Δe)**:** The rate of change of the error.

Output Variables:
The fuzzy controller generates control actions to adjust the DAB converter's operation. These typically involve:

- Duty Cycle (D)**:** The duty cycle of the converter switches that control the power delivered to the battery.
- Switching Frequency (f)**:** The frequency at which the converter operates to regulate power delivery.

Fuzzy Membership Functions: Each input and output is assigned a set of fuzzy membership functions that define how values are mapped to fuzzy sets. These membership functions define categories such as:

- Low, Medium, High for current or voltage levels.
- Positive, Zero, Negative for errors and changes in error.

Rule Base: The fuzzy controller uses a set of linguistic rules (typically formulated from expert knowledge) to map the inputs to the outputs. For instance, if the error in voltage is high, the controller might increase the duty cycle to reduce the error. An example rule could be:

- If Error is Positive and Change in Error is Positive, then increase the duty cycle.
- If Error is Zero, then keep the duty cycle unchanged.

Defuzzification: After applying the fuzzy rules, the fuzzy controller outputs a crisp control value (e.g., a duty cycle) through defuzzification. The most common method for defuzzification is the **centroid method**, where the controller computes the center of gravity of the fuzzy output set.

6. MATHEMATICAL CALCULATIONS INVOLVED

Voltage and Current Relationship in the DAB Converter: The DAB converter is a **DC-DC** converter, and the relationship between the input and output voltage and current can be expressed as:

$$V_{\text{out}} = \frac{V_{\text{in}} \cdot D}{1 - D}$$

Where:

- Vout is the output voltage (battery voltage),
- Vin is the input voltage (from solar panels or grid),
- D is the duty cycle of the converter switches.

This equation governs the basic operation of the DAB converter, where the duty cycle DDD is adjusted based on the battery voltage and charging current.

Charging Current Control: The current charging profile is typically governed by the **CC-CV (Constant Current Constant Voltage)** method for charging Lithium-Ion batteries. During the constant current phase, the charging current Ichargeremains fixed, and during the constant voltage phase, the current decreases as the battery approaches full charge.

The relationship for the charging current can be expressed as:

$$I_{\text{charge}} = I_{\text{max}} \cdot \left(1 - \frac{V_{\text{out}}}{V_{\text{max}}}\right)$$

Where:

- Imax is the maximum charging current (constant during the CC phase),
- Vmax is the maximum voltage the battery can reach (usually 4.2V per cell for Li-ion batteries),

- Voutis the actual output voltage.
- The charging current is then adjusted based on the desired constant voltage (CV) threshold.

Fuzzy Control Law

The fuzzy control algorithm can be represented as a function of the error (eee) and the change in error (Δe):

$$D = f(e, \Delta e)$$

Where DDD is the duty cycle, and eee and Δe\Delta eΔe are the error and the change in error of the battery voltage, respectively. The fuzzy rules govern how the duty cycle adjusts based on these variables.
For instance, a typical rule might be:

$$\text{If } e \text{ is large and } \Delta e \text{ is large, then increase } D.$$

The defuzzification process is applied to obtain a crisp value for the duty cycle that will regulate the converter's operation.

Energy Stored in Battery

The energy stored in the battery during charging can be calculated using:

$$E = \int_0^T P(t)\,dt = \int_0^T V_{\text{battery}}(t) \cdot I_{\text{battery}}(t)\,dt$$

Where:

- E is the energy stored in the battery,
- P(t) is the instantaneous power delivered to the battery,
- Vbattery(t) is the battery voltage at time t,
- Ibattery(t) is the charging current at time t,
- TTT is the charging time.

By controlling the voltage and current precisely, the fuzzy controller ensures that the battery receives power in a controlled manner, minimizing the risk of overcharging and overheating.

7. FUZZY LOGIC CONTROLLER AND MATHEMATICAL CALCULATIONS FOR THE MODIFIED DAB CONVERTER TOPOLOGY

The Dual Active Bridge (DAB) converter is often employed in fast Electric Vehicle Charging Stations (EVCS) for bidirectional power transfer, particularly in DC microgrid-connected systems. However, in the fast charging process, unstable dynamics such as overshoot or resonance can negatively affect the charging performance and degrade the EV battery's lifespan. This issue becomes more critical in high charging currents and fast charging rates, making it essential to stabilize the system to ensure proper charging without battery degradation. The proposed topology and control scheme address these issues through active damping, and fuzzy logic control can be employed to further refine the system's dynamic response, ensuring smooth and stable power delivery.
Fuzzy Logic Controller (FLC) Design in DAB Converter

The Fuzzy Logic Controller (FLC) helps in controlling the behavior of the DAB converter during the charging and discharging of EV batteries. The primary role of the FLC in this context is to ensure that the charging current and voltage remain within safe operating limits, mitigating overshoot and preventing rapid fluctuations during fast charging.

Input Variables for Fuzzy Logic Controller:

- Error in Voltage (e): The difference between the desired battery voltage and the actual output voltage from the converter.
- Change in Error (Δe): The rate of change of the voltage error, helping the controller to decide whether to increase or decrease the duty cycle.
- Battery Current (I): Helps in monitoring the charging current to ensure that it stays within the set boundaries, particularly important during fast charging.

Output Variables:

- **Duty Cycle (D)**: The percentage of time the switches in the DAB converter are on, which controls the amount of power transferred to the battery.
- **Switching Frequency (f)**: The frequency at which the switches in the converter operate to maintain efficiency while preventing overshoot.

Fuzzy Rules: The fuzzy rules are designed based on the input variables to adjust the duty cycle and switching frequency. For example:

- If the error is large and the change in error is positive, the controller will increase the duty cycle to reduce the error.
- If the error is zero, the controller will keep the duty cycle constant to maintain stable charging.
- If the current exceeds a threshold, the controller will adjust the switching frequency to avoid excessive heating.

Defuzzification: After evaluating the fuzzy rules, the output is defuzzified to a crisp value (e.g., the duty cycle), which is then used to adjust the DAB converter's operation.
Mathematical Analysis: Bode Plot and Stability in DAB Converter the Bode plot provides valuable insight into the stability of the system by showing the frequency response of the open-loop transfer function (TF). For both voltage control mode and current control mode, the Bode plots of the system with active damping (incorporating the Notch Filter (NF)) are plotted in Fig. 10.

- **Voltage Control Mode**: In this mode, the control algorithm adjusts the duty cycle to maintain a constant battery voltage. The Bode plot shows the frequency response of the system in this mode, highlighting the system's ability to reject disturbances and maintain a stable voltage under varying load conditions.
- **Current Control Mode**: This mode maintains a constant current during the charging process. The Bode plot in this mode reveals how effectively the system can regulate current while minimizing oscillations that could negatively impact the battery.

The inclusion of **active damping** helps attenuate resonance frequencies, reducing **overshoot** and enhancing system stability. The transfer functions (TF) for the voltage and current control modes are given by equations (31) and (32) in the original work.

Mathematical Formulation for the Damping and Stability:

The damping introduced by the notch filter (NF) reduces the unstable dynamics observed at the resonance frequency:

$$TF_{\text{voltage}} = \frac{K_{\text{voltage}}}{s^2 + 2\zeta\omega_n s + \omega_n^2}$$

Where:

- Kvoltage is the gain for the voltage control mode,
- ωn is the natural frequency of the system,
- ζis the damping factor.

$$TF_{\text{current}} = \frac{K_{\text{current}}}{s^2 + 2\zeta\omega_n s + \omega_n^2}$$

Where:

Kcurrentis the gain for the current control mode.

8. SIMULATION AND PERFORMANCE EVALUATION

The system's performance is evaluated through **Simulink simulations** (MATLAB R2022a), where the system is tested for a **nominal resistive load** of 14.44 Ω. The simulation results (Fig. 15 to 19) show that:

- The primary and secondary bridge voltages, as well as the coupling inductor current (I1), are displayed in the waveform (Fig. 15).
- The Zero Voltage Switching (ZVS) condition for both primary and secondary bridges is achieved, improving the efficiency (Fig. 16).
- The converter's efficiency curve (Fig. 17) demonstrates that the DAB converter operates at 96.1% efficiency at rated load conditions.

Battery Charging with CCCV Algorithm

To implement fast charging, the battery is connected with a nominal voltage (VBatt) of 320 V and a capacity of 13 Ah, and it is charged at a 2C rate using the Constant Current Constant Voltage (CCCV) algorithm. The State of Charge (SoC) and other battery parameters are tracked during the charging process under varying C-rates.

- State of Charge (SoC): The SoC of the battery is monitored and gradually increases from 10% to 66% as shown in the simulation results (Fig. 18).
- Current and Voltage Tracking: The dynamic response of the system is observed, and the phase shift between the voltage and current is adjusted based on the changing C-rate.
- Mathematical Calculation for Battery Charging: For the 2C charge rate, the charging current Ichargeis:

$$I_{\text{charge}} = 2 \times C_{\text{capacity}} = 2 \times 13\,\text{Ah} = 26\,\text{A}$$

This ensures a rapid charge, and the CCCV algorithm ensures that the voltage does not exceed safe limits, protecting the battery from overcharging.

System Robustness and Bode Analysis

The **robustness** of the system is validated through Bode plot analysis**,** where the system's response to parameter variations in the LC filter is plotted. Figures 12 and 13 confirm that even with ±10% variations in the filter parameters, no overshoot occurs, demonstrating the system's ability to handle parameter mismatches effectively.
Bidirectional Operation (G2V and V2G Modes)
The system also supports bidirectional power flow, allowing for Vehicle-to-Grid (V2G) and Grid-to-Vehicle (G2V) operation. In the V2G mode, the battery is discharged at a 1C rate, and the SoC drops from 50% to 25%**.** The current in the DC link (I_s) remains constant during this operation, as shown in the waveform in Fig. 21.

9. CONCLUSION

The fuzzy logic control and active damping techniques implemented in the proposed DAB converter topology for fast EV charging systems ensure optimal performance, stability, and efficiency. The Bode analysis and simulations confirm the system's ability to mitigate overshoot and ensure smooth voltage and current regulation during fast charging. By achieving Zero Voltage Switching (ZVS) and maintaining a 96.1% efficiency, the system is well-suited for fast and safe EV battery charging, with minimal degradation over time. The bidirectional power flow capability, verified through simulations and real-time implementations, demonstrates the system's robustness and flexibility in varying operational conditions. This research contributes to the development of sustainable and efficient EV charging infrastructure, enhancing battery health and longevity while facilitating the integration of renewable energy sources into the grid.

REFERENCES

[1]. I. Kholiq, "PEMANFAATAN ENERGI ALTERNATIF SEBAGAI ENERGI TERBARUKAN UNTUK MENDUKUNG SUBTITUSI BBM," no. 2, p. 17, 2015.
[2]. B. H. Purwoto, "EFISIENSI PENGGUNAAN PANEL SURYA SEBAGAI SUMBER ENERGI ALTERNATIF," Emit. J. Tek. Elektro, vol. 18, no. 01, pp. 10–14, Mar. 2018, doi: 10.23917/emitor.v18i01.6251.
[3]. N. K. Raghavendra and K. Padmavathi, "Solar Charge Controller for Lithium-Ion Battery," in 2018 IEEE International Conference on Power Electronics, Drives and Energy Systems (PEDES), Chennai, India, Dec. 2018, pp. 1–5, doi: 10.1109/PEDES.2018.8707743.
[4]. H. Suryoatmojo, "Design Li-Po Battery Charger with Buck Converter under Partially CC-CV Method," in 2020 International Seminar on Intelligent Technology and Its Applications (ISITIA), Surabaya, Indonesia, Jul. 2020, pp. 101–106, doi: 10.1109/ISITIA49792.2020.9163754.
[5]. A. Tomaszewska et al., "Lithium-ion battery fast charging: A review," eTransportation, vol. 1, p. 100011, Aug. 2019, doi: 10.1016/j.etran.2019.100011.
[6]. T. Andromeda et al., "Design of DC Fast Charging Buck Converter for LFP Battery on Electric Car," in 2019 6th International Conference on Electric Vehicular Technology (ICEVT), Bali, Indonesia, Nov. 2019, pp. 258–262, doi: 10.1109/ICEVT48285.2019.8993974.

[7]. H. Matalata and L. W. Johar, "ANALISA BUCK CONVERTER DAN BOOST CONVERTER PADA PERUBAHAN DUTY CYCLE PWM DENGAN MEMBANDINGKAN FREKUENSI PWM 1,7 Khz DAN 3,3 Khz," J. Ilm. Univ. Batanghari Jambi, vol. 18, no. 1, p. 42, Feb. 2018, doi: 10.33087/jiubj.v18i1.431.

[8]. S.-C. Wang, Y.-L. Chen, Y.-H. Liu, and Y.-S. Huang, "A fast-charging pattern search for li-ion batteries with fuzzy-logic-based Taguchi method," in 2015 IEEE 10th Conference on Industrial Electronics and Applications (ICIEA), Auckland, New Zealand, Jun. 2015, pp. 855– 859, doi: 10.1109/ICIEA.2015.7334230.

[9]. A. Al-Refai, R. AbouSleiman, and O. A. Rawashdeh, "A programmable charger for monitoring and control of multi-cell lithiumion batteries," in 2012 IEEE National Aerospace and Electronics Conference (NAECON), Dayton, OH, USA, Jul. 2012, pp. 68–74, doi: 10.1109/NAECON.2012.6531031.

[10]. M. M. Hoque, M. A. Hannan, and A. Mohamed, "Optimal CC-CV charging of lithium-ion battery for charge equalization controller," in 2016 International Conference on Advances in Electrical, Electronic and Systems Engineering (ICAEES), Putrajaya, Malaysia, Nov. 2016, pp. 610–615, doi: 10.1109/ICAEES.2016.7888119.

